Neuronal Nogo-A negatively regulates dendritic morphology and synaptic transmission in the cerebellum

Marija M. Petrinovic[a,b,1,2], Raphael Hourez[c], Elisabeth M. Aloy[a,b], Gregoire Dewarrat[a,b], David Gall[c], Oliver Weinmann[a,b], Julien Gaudias[d], Lukas C. Bachmann[a,b], Serge N. Schiffmann[c], Kaspar E. Vogt[d], and Martin E. Schwab[a,b,2]

[a]Brain Research Institute, University of Zürich, 8057 Zürich, Switzerland; [b]Department of Health Sciences and Technology, ETH Zürich, 8057 Zürich, Switzerland; [c]Laboratoire de Neurophysiologie, Université Libre de Bruxelles, 1070 Brussels, Belgium; and [d]Division of Pharmacology and Neurobiology, Biozentrum, University of Basel, 4056 Basel, Switzerland

Neuronal signal integration as well as synaptic transmission and plasticity highly depend on the morphology of dendrites and their spines. Nogo-A is a membrane protein enriched in the adult central nervous system (CNS) myelin, where it restricts the capacity of axons to grow and regenerate after injury. Nogo-A is also expressed by certain neurons, in particular during development, but its physiological function in this cell type is less well understood. We addressed this question in the cerebellum, where Nogo-A is transitorily highly expressed in the Purkinje cells (PCs) during early postnatal development. We used general genetic ablation (KO) as well as selective overexpression of Nogo-A in PCs to analyze its effect on dendritogenesis and on the formation of their main input synapses from parallel (PFs) and climbing fibers (CFs). PC dendritic trees were larger and more complex in Nogo-A KO mice and smaller than in wild-type in Nogo-A overexpressing PCs. Nogo-A KO resulted in premature soma-to-dendrite translocation of CFs and an enlargement of the CF territory in the molecular layer during development. Although spine density was not influenced by Nogo-A, the size of postsynaptic densities of PF–PC synapses was negatively correlated with the Nogo-A expression level. Electrophysiological studies revealed that Nogo-A negatively regulates the strength of synaptic transmission at the PF–PC synapse. Thus, Nogo-A appears as a negative regulator of PC input synapses, which orchestrates cerebellar connectivity through regulation of synapse morphology and the size of the PC dendritic tree.

The ability of a neuron to integrate into neuronal networks and process information is determined by the size and shape of its dendritic arbor. Dendritic spines contribute importantly to synaptic function and plasticity (1). The molecular mechanisms controlling these parameters are not fully understood. In addition to neurotransmitters and activity-related signaling systems, classes of molecules that are known to regulate neurite outgrowth and their receptors have been implicated in dendritic and/or spine growth and plasticity (2).

An important negative regulator of neurite outgrowth is the membrane protein Nogo-A (3). Whereas the growth inhibitory function of Nogo-A in the injured central nervous system (CNS) is well documented (4, 5), only few studies have addressed its physiological roles (3, 6, 7). Recent observations also point to functions of Nogo-A at synapses: overexpression of Nogo-A in adult Purkinje cells (PCs) induces synapse disassembly (8), whereas the overexpression of its receptor NgR1 leads to impairments in long-term memory (3). Nogo-A and both known Nogo receptors, NgR1 and paired immunoglobulin-like receptor B (PirB), negatively modulate hippocampal long-term potentiation (LTP) (9–11). NgR1 and PirB are also involved in the restriction of developmental, activity-driven plasticity in the visual cortex (3).

In addition to its mainly glial expression in the adult CNS (12, 13), Nogo-A is expressed by many central and peripheral neurons where its levels are high during development but lower or undetectable in the adult (3). In rodent cerebellum Nogo-A and

NgR1 are expressed in a complementary manner: Nogo-A is mainly present in PCs, whereas the granule cells (GCs) are a main site of NgR1 expression (14–16). The time course of high Nogo-A expression in PCs correlates with the time of PC dendritogenesis, climbing fiber (CF)–PC synapse refinement and parallel fiber (PF)–PC synapse development (6, 8, 14). These findings suggest that Nogo-A could play a role in the regulation of PC connectivity.

Nogo-A knockout (KO) mice and transgenic mice (TG) overexpressing Nogo-A exclusively in PCs under the L7 promoter (L7–Nogo-A TG), revealed in the present study that Nogo-A acts as a negative regulator of the size and complexity of the PC dendritic arbor as well as of the size and strength of the PF synapses. In addition, genetic ablation of Nogo-A influences the establishment of CF innervation on the PC dendrites. These results identify a distinct biological function for Nogo-A expressed by neurons for the development of synaptic connections in the cerebellum.

Results

Four types of mice were used in this study: Nogo-A KO and wild-type (WT) mice of C57BL/6 background and L7–Nogo-A TG mice, which overexpress Nogo-A only in PCs (8), and their corresponding WT controls of FVB/N background. To account for strain differences (17) we always compared mutant animals with the WT mice of the corresponding strain. As the cerebellar lobules, and even different regions of the same lobule, mature at different time points (18, 19), we always analyzed the bank and gyrus subdivisions of the lobules IV/V, VI/VII, and IX.

Nissl staining showed no differences between the mutants and the WT animals with regard to the size, foliation, laminar organization, and histology of the cerebellum (Fig. S1A). No obvious differences in PC arrangement and their calbindin immunoreactivity were noted between the four lines of mice (Fig. S1B). Western blot (WB) analysis of cerebella at postnatal day (P) 28 revealed comparable Nogo-A and -B expression in WT mice of both strains (Fig. S2A). Nogo-A KO mice had elevated levels of Nogo-B as described earlier (20) (Fig. S2A). WB with the antibody 3D11, which is specific for the Nogo-A transgene of rat origin (21), confirmed the overexpression of Nogo-A in cerebellar

NEUROSCIENCE

lysates of P28 L7–Nogo-A TG mice (Fig. S2B). Protein levels of NgR1 were equal in all four groups of mice (Fig. S2C).

Distribution of Nogo-A and NgR1 in the Cerebellum. At P28, Nogo-A was found only in PC bodies, dendrites, and their spines (Fig. 1A). Double labeling with anti-NgR1 and anti-vesicular glutamate transporter 1 (anti-VGluT1) antibodies demonstrated a strong expression of NgR1 in PF terminals (Fig. 1B), whereas colabeling with antibodies against calbindin and NgR1 revealed very weak expression of NgR1 in PC bodies (Fig. S2D). The presence of Nogo-A in the postsynaptic PC spines and of NgR1 in the presynaptic PF terminals was confirmed by immunoelectron microscopy (Fig. S3 A and B).

Nogo-A expression in the PCs is developmentally regulated (6, 14). Our WB analysis confirmed a weak expression of Nogo-A in the cerebellum of WT mice during the first postnatal week, followed by a fivefold up-regulation by P14 (Fig. S3C). Similar pattern of Nogo-A expression was observed in L7–Nogo-A TG mice, in line with the notion that the L7 promoter is fully activated only in the second postnatal week (22) (Fig. S3D). With the progression of development, the Nogo-A gets down-regulated in WT mice to ∼25% of the level at P14 (Fig. S3C). No down-regulation occurred in L7–Nogo-A TG mice (Fig. S3D). Developmental regulation of Nogo-A expression in PCs was confirmed by immunohistochemistry (IHC) (Figs. S1B and S3E).

Nogo-A Negatively Regulates PC Dendritic Tree Morphology and Input Synapses. For a morphometric analysis, P28 PCs were filled with biocytin. The overall cellular volume was increased in Nogo-A KO PCs (Fig. 2 A and B), with both an increase in size (μm^3) of the somatic (WT/B: 5,288 ± 298 and KO: 6,629 ± 368; $P < 0.01$) and the dendritic (WT/B: 32,956 ± 2,994 and KO: 47,996 ± 4,317; $P < 0.01$) compartment. Overexpression of Nogo-A in PCs led to a decrease in their cellular volume (μm^3) (Fig. 2 A and B); both the somatic (WT/F: 6,265 ± 316 and TG: 5,237 ± 261; $P < 0.05$) and the dendritic (WT/F: 45,754 ± 4,418 and TG: 31,890 ± 2,219; $P < 0.05$) compartments were affected. The observed modifications of the dendritic tree volume could be a consequence of changes in the thickness, length, and/or complexity of dendrites. The average width of distal dendritic segments was enlarged in the Nogo-A KO and reduced in the L7–Nogo-A TG PCs (Fig. 2B). The length (μm) of the primary dendrites (the main, central dendrites, directly connected to the cell body of PCs) was also negatively influenced by Nogo-A (WT/B: 140.32 ± 7.63 and KO: 167.69 ± 9.86; $P < 0.05$; WT/F: 132.32 ± 8.93 and TG: 106.84 ± 12.97; $P < 0.05$). To assess the complexity of the
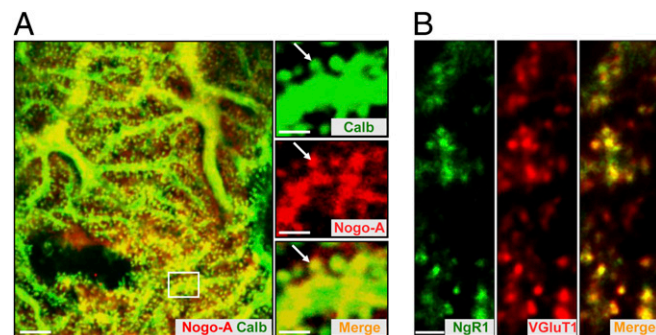

Fig. 2. Nogo-A negatively regulates PC dendritic tree morphology and affects electrophysiological properties of PCs. (A) Confocal images of biocytin-filled PCs from cerebellar slices of P28 Nogo-A KO, L7–Nogo-A TG and the corresponding WT mice. Note the larger dendritic arbor of the Nogo-A KO PC compared with its WT/BL6 control and the less complex arbor and a smaller cell body of the Nogo-A overexpressing PCs compared with strain-matched WT controls. (Scale bars, 50 μm.) (B) Nogo-A negatively regulates the total cell volume, width of distal dendritic segments, and the length of PSDs. Whereas Nogo-A KO exerts no effect on the 2D fractal dimension, overexpression of Nogo-A reduces the complexity of PC dendritic arbors (B). (C and D) Nogo-A regulates the spontaneous firing activity of P28 PCs, as well as the action potential half-width. (E and F) Current–frequency plots and corresponding histograms demonstrate that Nogo-A KO has no effect on PC intrinsic excitability (E), whereas its overexpression leads to an increase of the intrinsic neuronal excitability compared with WT controls (F). Values represent means ± SEM of 11–26 cells (three to six mice) per genotype; *$P < 0.05$, **$P < 0.01$, ***$P < 0.001$, Student t test.

PC dendritic tree, we used a 2D fractal analysis. Whereas Nogo-A KO PCs were not significantly different from WT controls, those overexpressing Nogo-A demonstrated a significant decrease in 2D fractal dimension (Fig. 2B). PKCγ, which has been suggested to play a role in dendritic growth and differentiation of PCs (23), was down-regulated in the Nogo-A KO and doubled in the L7–Nogo-A TG mice (Fig. S4 A and B). These results suggest that Nogo-A negatively modulates PC size and the complexity of its dendritic tree.

Spine density showed no abnormalities in PCs either lacking (WT/B: 2.90 ± 0.20 and KO: 2.30 ± 0.70; $P = 0.58$) or over-expressing (WT/F: 1.73 ± 0.09 and TG: 1.74 ± 0.24; $P = 1.00$) Nogo-A. This absence of change in spine density, combined with the differing size of the dendritic tree, points to a negative

Fig. 1. Distribution of Nogo-A and NgR1 in the cerebellum. (A and B) Nogo-A and its receptor NgR1 are complementarily expressed at synaptic sites in the cerebellum of P28 WT/BL6 mice. (A) Double immunolabeling with anti-calbindin (green) and anti–Nogo-A (red) antibodies revealed the presence of Nogo-A in dendrites and spines (arrows) of PCs. Higher power micrographs correspond to the boxed region. (Scale bars, 5 μm; 2 μm in *Insets*.) (B) Colabeling with antibodies against NgR1 (green) and VGluT1 (red) demonstrates the strong expression of NgR1 in the presynaptic, VGluT1+ PF terminals. (Scale bar, 2 μm.)
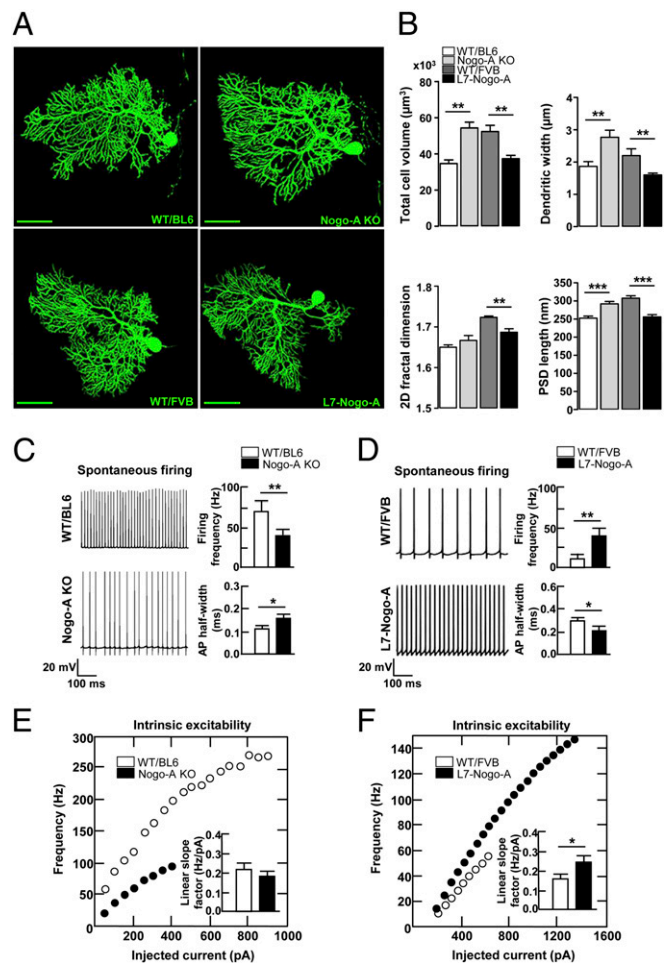
regulation of the total spine number by Nogo-A. To analyze a key functional component of spine synapses, the postsynaptic density (PSD), we used electron microscopy (EM). At P28, the average length of the PSD, a measure that is well correlated with the spine head volume and the strength of synaptic transmission (1), was increased in Nogo-A KO and reduced in L7–Nogo-A TG compared with WT PCs (Fig. 2B). Similar changes in the PSD length (nm) were also observed in 5-mo-old mutant mice (WT/B: 275.60 ± 4.95 and KO: 321.41 ± 5.43; $P < 0.001$; WT/F: 346.91 ± 7.12 and TG: 269.20 ± 6.38; $P < 0.001$). Biochemically, glutamate receptors, CamKII, PSD95 and Homer, are major constituents of PSDs (24). WB and IHC evaluation demonstrated negative correlation between these PSD components and the expression level of Nogo-A in the molecular layer (ML) of P28 mice (Figs. S4 A and B and S5 A and B).

Electrophysiological Properties of PCs Are Affected by Nogo-A. Alterations in Nogo-A content affected neither the resting membrane resistance (MΩ) (WT/B: 146 ± 19 and KO: 170 ± 22; $P = 0.47$; WT/F: 218 ± 31 and TG: 232 ± 54; $P = 0.76$) nor the minimal membrane potential (mV) measured during spontaneous activity (WT/B: -54.5 ± 1.7 and KO: -56.4 ± 1.0; $P = 0.38$; WT/F: -63.9 ± 1.6 and TG: -67.6 ± 1.6; $P = 0.63$). The spontaneous firing rate was positively correlated with Nogo-A level (Fig. 2 C and D). In addition, Nogo-A KO PCs showed a ~30% increase in the action potential half-width evaluated at the threshold potential where fast repetitive spiking is obtained (Fig. 2C), whereas a commensurate ~30% decrease of action potential half-width was observed in L7–Nogo-A TG PCs (Fig. 2D).

Intrinsic neuronal excitability, which is well correlated with the spontaneous firing frequency, was investigated by holding the membrane potential at -80 mV and injecting steps of depolarizing current from 0 to 2.5 nA with 50-pA increments. Whereas intrinsic excitability was slightly, although not significantly reduced in Nogo-A KO PCs (Fig. 2E), it was significantly enhanced in L7–Nogo-A TG PCs compared with WT cells (Fig. 2F).

Genetic Ablation of Nogo-A Affects the Developmental Rearrangement of CF Terminals on PCs. The reduction of poly- to single CF innervation of PCs has long been a model for developmental synapse elimination (25). In mice, pruning of surplus CF connections finishes by the end of the third postnatal week, leaving ~90% of the PCs innervated by only one CF (26). Simultaneously, the CF terminals translocate from the PC somata to the proximal dendrites (25, 27). Developmental up-regulation of Nogo-A coincides with the time of both somatodendritic translocation and elimination of supernumerary CFs, suggesting its possible involvement in the regulation of the synapse refinement processes in the cerebellum.

Quantification of VGluT2$^+$ CF terminals at early developmental stages (P4–P7), i.e., before the onset of synapse elimination, revealed a higher density of CF terminals in the ML of Nogo-A KOs, whereas no difference was observed between L7–Nogo-A TG mice and their WT controls (Fig. 3 B and C). At P14, a stage when ~50% of WT PCs bear only one CF, the average density (terminals per mm^2) of VGluT2$^+$ puncta in the ML was again higher in the Nogo-A KO mice (WT/B: $14{,}320 \pm 831.9$ and KO: $18{,}960 \pm 622.0$; $P < 0.001$), whereas the overexpression of Nogo-A showed no effect (WT/F: $14{,}940 \pm 310.1$ and TG: $15{,}250 \pm 411.7$; $P = 0.34$). At 4 wk, when the synaptic rearrangement should be finished, the density of VGluT2$^+$ terminals in Nogo-A KOs was ~50% higher than in WT mice, whereas no abnormalities were observed in L7–Nogo-A TG mice (Fig. 3 A and D). A WB analysis confirmed the increase in the amount of VGluT2 protein in the ML of P28 Nogo-A KOs, and no detectable change in its expression in the cerebella of L7–Nogo-A TGs compared with WT controls (Fig. S4 A and B). In adult (P60) mice the VGluT2 immunostaining pattern showed a comparable density of CF terminals in mutant mice and their WT controls (Fig. 3E).

We further analyzed the CF innervation patterns in P28 Nogo-A KO mice by labeling a small fraction of CFs with biotinylated dextran amine (BDA) and counterstaining the sections for VGluT2 and calbindin. In both WT and Nogo-A KO mice, all PC bodies contacted by BDA$^+$ CF showed a complete overlap of BDA and VGluT2 staining and an absence of BDA$^-$ CF terminals, which would have originated from additional, non–BDA-labeled CFs (Fig. S6A). Thus, multiply innervated PCs were not detectable by this method. CF innervation of PCs was also analyzed by electrophysiological measurements: CFs were stimulated in the GC layer of sagittal cerebellar slices from P28 Nogo-A KO mice and their WT littermates. As the stimulus intensity was gradually increased, a typical large excitatory postsynaptic current (EPSC) was elicited in an all-or-none fashion in the majority of the PCs, indicating that these PCs are innervated by a single CF in WT and Nogo-A KO PCs (Fig. S6 B and C). In ~11% of WT and ~4% of Nogo-A KO PCs CF-mediated EPSCs had two discrete steps when the stimulus intensity was above the threshold, suggesting that these cells had one supernumerary CF in addition to the main CF (Fig. S6 B and C). Thus, the higher density of VGluT2$^+$ CF terminals observed in P28 Nogo-A KO PCs points to a hyperinnervation emerging from a single inferior olive axon.

During normal cerebellar maturation, CF contacts shift from the soma to the dendrites as PCs elaborate their dendritic arbor. Whereas the somatodendritic translocation of CF contacts occurred to an equivalent extent in the WT and the L7–Nogo-A TG cerebella, significant differences were found between WT and Nogo-A KO mice (Fig. S7 A and B). At P14 Nogo-A KO mice had more PCs without any VGluT2$^+$ dots on their soma (Fig. S7B), but fewer PCs with more than six VGluT2$^+$ dots on their soma than their WT littermates (Fig. S7B), indicating either precocious somatodendritic translocation or, alternatively, an earlier start of CF–PC synapse refinement. To distinguish these possibilities, we performed anterograde labeling of CFs with BDA combined with immunofluorescence for VGluT2 and calbindin in addition to electrophysiological recordings of CF EPSCs. All polyinnervated Nogo-A KO and WT PCs had comparable numbers of BDA$^+$/VGluT2$^+$ and BDA$^-$/VGluT2$^+$ CF terminals on their somata (BDA$^+$/VGluT2$^+$: WT/B, 3.21 ± 0.38 and KO, 4.32 ± 0.27; $P = 0.89$; BDA$^-$/VGluT2$^+$: WT/B, 3.60 ± 0.22 and KO, 2.8 ± 0.19; $P = 0.74$) (Fig. S7C). Similarly, electrophysiological measurements showed that the percentage of P14 PCs displaying either single or dual CF innervation was comparable between WT (23% dually innervated PCs; $n = 6/26$) and Nogo-A KO mice (17% dually innervated PCs, $n = 5/29$) (Fig. S7 D and E). Thus, both approaches excluded the possibility of an earlier start of synapse elimination in the absence of Nogo-A.

Precocious translocation of CF contacts from the soma to the dendrites of PCs was further confirmed by an increase in the extent (%) of the CF innervation territory in Nogo-A KO mice (P14: WT/B, 59.03 ± 2.11 and KO, 74.12 ± 1.42; $P < 0.05$; P28: WT/B, 79.09 ± 1.19 and KO, 92.24 ± 1.15; $P < 0.05$) (Fig. 3A and Fig. S6A, arrows). No genotypic differences were observed with regard to the total thickness (μm) of the ML at P28 (WT/B, 178.21 ± 8.92 and KO, 183.65 ± 12.14; $P = 0.46$; WT/F, 167.18 ± 10.67 and TG, 172.49 ± 9.84; $P = 0.72$). In the adult (P60) Nogo-A KO (WT/B, 88.40 ± 1.73 and KO, 90.28 ± 1.06; $P = 0.74$) as well as in the developing and adult L7–Nogo-A TG mice, the CF innervation territory (%) was comparable with that of WT controls (P14: WT/F, 58.21 ± 1.42 and TG, 61.64 ± 1.53; $P = 0.36$; P28: WT/F, 84.38 ± 1.33 and TG, 82.85 ± 1.78; $P = 0.63$; and P60: WT/F, 91.12 ± 1.12 and TG, 90.75 ± 1.13; $P = 0.75$) (Fig. 3A). Thus, deletion of Nogo-A enhances the translocation and spread of CF terminals along the dendritic tree and leads to a temporary hyperinnervation of the PCs.

Nogo-A Affects the PF–PC Synapse Number and Synaptic Transmission. The density of the VGluT1$^+$ PF terminals was determined in the ML of P14, P28, and P60 mice; it was negatively correlated with Nogo-A expression level at all three developmental stages
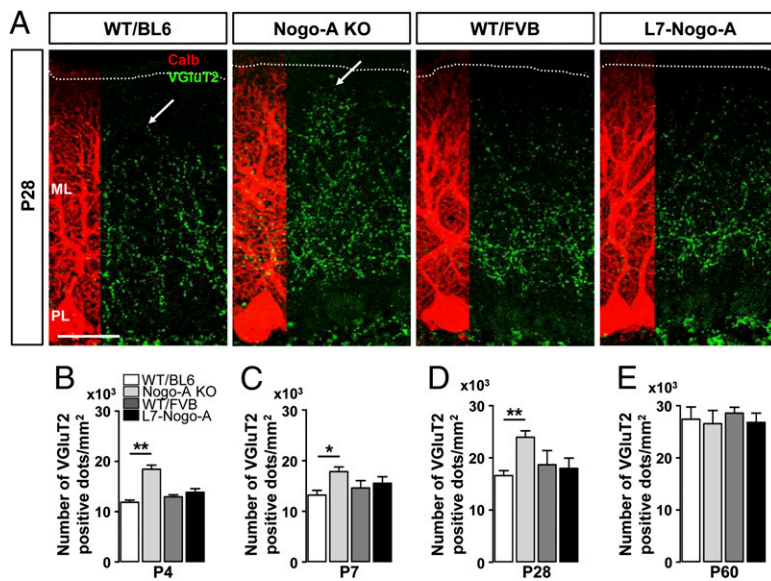
Fig. 3. Genetic deletion of Nogo-A affects the developmental rearrangement of CF terminals on PC dendrites. (*A*) Confocal images of VGluT2+ CF terminals (green) on P28 PCs stained for calbindin (red). Note the increased territory of CF synapses in Nogo-A KO mice at P28 (arrows). Dotted lines indicate the pial surface. ML, molecular layer; PL, PC layer. (Scale bar, 50 μm.) An increase in the density of VGluT2+ CF varicosities was found in Nogo-A KO mice at P4 (*B*), P7 (*C*), and P28 (*A* and *D*). This effect of Nogo-A KO on the CF innervation pattern was no longer visible at P60 (*E*). Overexpression of Nogo-A had no effect on either the density or the position of CF terminals (*A–E*). Values represent means ± SEM of 103–116 cells (six mice) per genotype; *P < 0.05, **P < 0.01, Student *t* test.

(Fig. 4 *A–D*). WB analysis of P28 mutant and WT mouse cerebellar lysates confirmed the negative correlation between the VGluT1 and Nogo-A expression levels (Fig. S4 *A* and *B*). Similarly to VGluT1, SNAP25, which is highly expressed in PF terminals (28), was up-regulated in Nogo-A KO and down-regulated in L7–Nogo-A TG mice (Fig. S4 *A* and *B*).

To test whether Nogo-A expression affects excitatory PF transmission, we measured EPSCs in the PCs in response to the electrical stimulation of a beam of PFs in P28 acute cerebellar slices of mutant and WT mice. Input–output relations measuring EPSC initial slope as a function of PF stimulus intensity were established for each recorded neuron. Because this relation is linear, we used the mean linear slope factor to compare the synaptic strength of the PF–PC synapses in mutant vs. WT mice. The synaptic strength for increasing PF stimulation was significantly increased in Nogo-A KO (Fig. 4 *E* and *G*) and decreased in L7–Nogo-A TG PCs compared with WT controls (Fig. 4 *F* and *H*). These results suggest an involvement of Nogo-A in the regulation of synaptic strength of the PF–PC synapses.

To determine whether Nogo-A acts pre- and/or postsynaptically we studied paired-pulse facilitation (PPF), a form of short-term synaptic plasticity associated with a change in the probability of glutamate release from the presynaptic PFs during a second stimulation that closely follows the first. PPF was elicited by twin pulses at different time intervals (5–245 ms in 2-ms increments) in L7–Nogo-A TG and control WT cells. The absence of a significant difference between mutant and WT cells (Fig. S8 *A* and *B*) suggests that the observed effects of Nogo-A on the synaptic strength are not likely due to regulations of glutamate release.

Discussion

Nogo-A expression in PCs reaches its peak during the second postnatal week and is afterward down-regulated to the low adult levels (8, 14). This time window correlates with the dendritic outgrowth of PCs, synapse formation, and refinement. The signaling pathways that regulate PC dendritic growth and complexity are poorly understood. Our morphological analysis showed that Nogo-A has a negative influence on the size of the PC bodies as well as the thickness, length, and complexity of PC dendrites. These results are well in line with previous studies in adult animals showing that Nogo-A is a negative regulator of the neuronal growth program (3, 29), as well as with the recent findings showing negative regulation of dendritic length and complexity by Nogo-A and NgR1 in hippocampal neurons (7, 30). PC dendrites are tightly packed and intermingled in the developing ML, and they were suggested to express NgR1 (31,

32). We speculate that they repulse each other mutually in a process of territorial sorting, whereby one repulsive/growth-restricting cue would be Nogo-A. Presence of NgR1 in the PC (31, 32) raises the possibility of its *cis*-interaction with Nogo-A in PC membrane, although such a mechanism has not been described for Nogo-A so far. Nevertheless, by binding to NgR1 or another yet unidentified receptor, Nogo-A activates the small GTPase RhoA (33), which has been shown to slow dendritic branch formation, yielding smaller and fewer branched dendritic arbors in various types of neurons (34). Notably, activation of RhoA has been recently identified as a mechanism by which NgR1 restricts dendritic growth and synapse formation in hippocampal neurons (30). Additionally, several studies have demonstrated that synaptic activity affects the dendritic arbor development (35, 36), thus opening the possibility that by negatively regulating synaptic transmission at PF–PC synapses, Nogo-A in turn negatively regulates dendritic growth.

Electrophysiological Properties of PCs Are Influenced by Nogo-A. The membrane resistance and the minimal membrane potential of PCs were not affected by Nogo-A. Alterations in excitability can be caused by a modification of cell volume/area as the cell capacitance will vary accordingly. Spontaneous firing rate was correlated with Nogo-A expression. In addition to the possible role of the Nogo-A–induced changes in the cell size, changes in the excitability and spontaneous firing rate of a neuron can be caused by the alteration in ionic conductances in the cell membrane (37). Previous studies (38, 39) suggested possible roles of Nogo-A for the regulation of Ca^{2+} and K^+ channels, which, in turn, have been considered to play a role in spontaneous firing of a neuron (37). All these results suggest that neuronal Nogo-A helps to maintain the PC output within a proper dynamic range, either by a regulatory influence on ion channels or indirectly through the modifications of the PC size and morphology. As neurons can increase their excitability to maintain a fixed level of firing output (40), the decrease in PF synaptic transmission in L7–Nogo-A TG mice may be compensated by the observed increase in intrinsic excitability of the PCs.

Nogo-A Influences the Maturation of the CF–PC Innervation. In the Nogo-A KO mice, the development of the CF input to PCs was disturbed: From P4 to P28 the number of CF terminals was increased by ∼35–55%, and they were distributed over larger areas of the ML. The disturbance seemed transitory, however, and no remaining polyinnervation of PCs could be detected. The absence
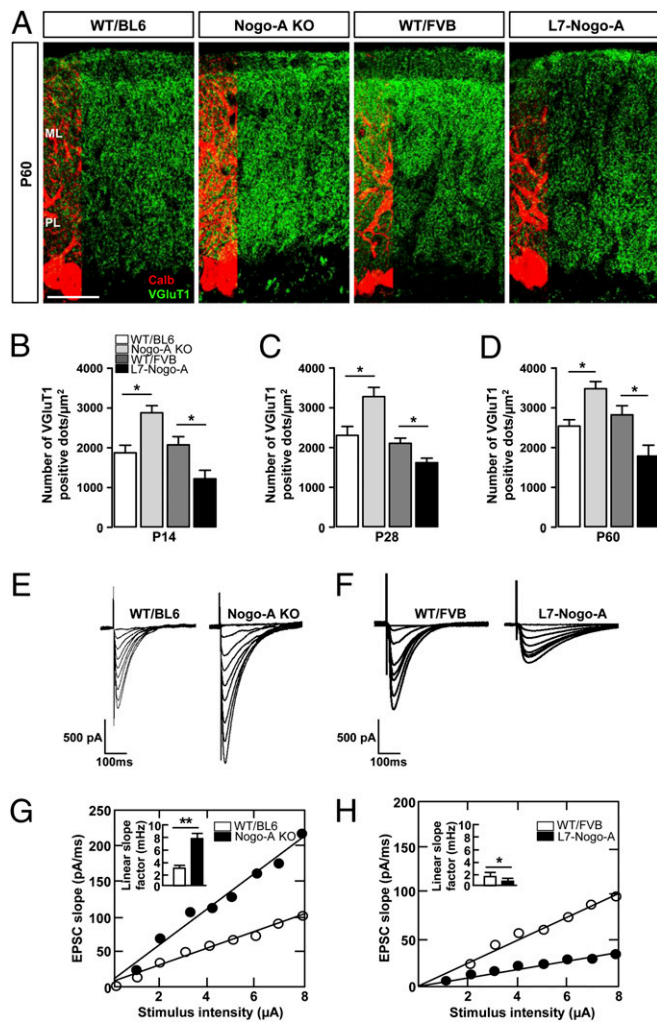
Fig. 4. Nogo-A negatively regulates the density and synaptic strength of the PF–PC synapses. (*A*) Confocal images of VGluT1⁺ PF terminals (green) on P60 PCs stained for calbindin (red). ML, molecular layer; PL, PC layer. (Scale bar, 50 μm.) Nogo-A KO leads to an increase in the number of PF terminals synapsing onto PC dendrites during development (*B* and *C*) as well as in the adult (*A* and *D*). Conversely, overexpression of Nogo-A in PCs resulted in a decrease in the number of PF terminations both during development (*B* and *C*) and in the adult (*A* and *D*). Values represent means ± SEM of 118–145 cells (six mice) per genotype; *$P < 0.05$, **$P < 0.01$, Student *t* test. (*E* and *F*) Typical input–output relationships obtained from P28 PCs in response to an increasing stimulation of PFs in Nogo-A KO (*E*), L7–Nogo-TG (*F*), and the corresponding WT mice. PCs of Nogo-A KO mice exhibit increased response to PF stimulation (*G*), whereas Nogo-A overexpression leads to a decrease in PC response to the same stimulus (*H*). Values represent means ± SEM of 19–25 cells (four to six mice) per genotype; *$P < 0.05$, **$P < 0.01$, Student *t* test.

of detectable effects of Nogo-A overexpression may be due to the late onset of the promoter used (22).

The molecular mechanisms that regulate CF synaptogenesis and fine tuning are not well understood. The GluRδ2, which probably acts as an adhesion molecule (41, 42), P/Q-type voltage-dependent Ca²⁺ channels, insulin-like growth factor (IGF), focal adhesion kinase (FAK), tyrosine-related kinase B (TrkB), myosinVa, glutamate transporter GLAST, a novel brain specific receptor-like protein family BSRP, mGluR1, the α subunit of the Gq subtype of GTP-binding protein, phospholipase Cβ4, and PKCγ were shown to play roles for the development of CF and PC connectivity (42–46). PKCγ, which has been shown to be activated by Nogo-A (47) was down-regulated in Nogo-A KO

and doubled in L7–Nogo-A TG mice, but its role in PC dendritic tree development seems rather complex (23, 48) and a possible role of this pathway for the observed effects of Nogo-A remains to be studied in detail. Importantly, several repulsive factors have also been identified to contribute to the synaptic specificity and synapse elimination in different CNS regions (49–52). In the maturing cerebellum, the mostly repulsive ephrin–Eph ligand-receptor family has been shown to guide olivo-cerbellar CF axons and influence their synapse and spine formation (53, 54). The present results show that the repulsive cell surface molecule Nogo-A influences CF synapse numbers, possibly by effects on synaptic pruning, and somatodendritic migration of the CF synapses. In light of the findings that functional differentiation of multiple CF inputs at P4–P7 is mainly based on an increase in the number of synaptic terminals supplied by each CF to the PC soma (55) it is tempting to speculate that the increase in the number of CF terminals observed in Nogo-A KO mice during the same time span contributes to the earlier establishment of the winning CF and thus its earlier translocation to PC dendrites. An increase in the number of the VGluT2⁺ CF terminals in P14–P28 Nogo-A KO mice could then be explained by the higher number of branches of the winning CF in Nogo-A KO mice and the longer time needed for their elimination.

Nogo-A Is a Negative Regulator of PF Synaptogenesis and Synaptic Transmission. The density of VGluT1⁺ PF terminals was increased in Nogo-A KO and decreased in L7–Nogo-A TG mice at P14–P60 compared with the WT controls. The results suggest that Nogo-A acts as a negative factor also for the formation of PF synapses, which starts in the second postnatal week, i.e., during the transient Nogo-A up-regulation in PCs. Importantly, this effect persisted into adulthood. Previous studies have shown the critical role for GluRδ2 and Cbln1 for selective strengthening of PF–PC synapses (45, 56). We also saw a significant increase in the PSD length in the P28 as well as in 5-mo-old Nogo-A KO mice and a decrease in the L7–Nogo-A TG animals. Several synaptic markers including GluR1, GluR2/3, Homer, PSD95, and CamKII showed corresponding changes.

Nogo-A is a potent repulsive molecule with destabilizing effects on the cytoskeleton of growth cones mediated by its downstream effectors RhoA/LIM Kinase (LIMK)/cofilin (3, 29). Actin and RhoA are enriched in presynaptic endings and in dendritic spines (57) and may link synaptic plasticity to actin and synaptic cytoskeleton remodeling (58). The negative correlation observed in the present study between the PF–PC synaptic length, the PF terminal number, and the expression level of Nogo-A may be due to such mechanisms. Alternatively, the changes in the PSD length observed after manipulation of the Nogo-A levels may be primarily a reflection of altered synaptic strength and activity, which leads to alterations in spine structure (35). The increase in the PSD length generally leads to spine stabilization, which may explain the enhanced motor learning observed in the Nogo-A KO mice (59). Conversely, in addition to the progressive loss of the inhibitory PC terminals, decreased length of the PSD and the consequent spine destabilization may be contributing to observed deficits in motor learning and coordination in the adult L7–Nogo-A TG mice (8).

The increased synaptic strength observed at the PF synapses of Nogo-A KO mice and the decreased transmission in the Nogo-A overexpressors at P28 are in line with the morphological and biochemical observations. The absence of a significant difference between WT and mutant animals in PPF suggests that the effects of Nogo-A on EPSC are not due to changes in presynaptic release mechanisms but are rather caused by the change in synapse number and/or size. Interestingly, it has been suggested that NgR1 restricts the synapse number in the developing hippocampus (30) and the enhancement of the hippocampal LTP was observed after Nogo-A neutralization or KO and in NgR1 KO mice (9–11). Whether acute suppression of Nogo-A or NgR1 in the adult cerebellum would also induce

NEUROSCIENCE

changes in PF function remains to be analyzed. The present results corroborate the role of Nogo-A as a negative controller of synaptic development, strength, and structure in several brain regions. In conclusion, the present results show that Nogo-A expressed by cerebellar PCs plays important roles for the development of these neurons and their input. Neuronal Nogo-A also influences, as a negative regulator, development, structure, and function of cerebellar synapses.

Materials and Methods

Nogo-A KO (pure C57BL/6 background) and L7-Nogo-A TG (in FVB/N background) mice of various developmental stages (P4-P60) were used in this study. WT mice of both C57BL/6 and FVB/N strains were used as respective controls. Detailed information on mutant animals, histology, IHC, electrophysiology, morphometric analysis of PCs and EM is provided in *SI Materials and Methods*.

1. Nimchinsky EA, Sabatini BL, Svoboda K (2002) Structure and function of dendritic spines. *Annu Rev Physiol* 64:313–353.
2. Jan YN, Jan LY (2003) The control of dendrite development. *Neuron* 40(2):229–242.
3. Schwab ME (2010) Functions of Nogo proteins and their receptors in the nervous system. *Nat Rev Neurosci* 11(12):799–811.
4. Schwab ME (2004) Nogo and axon regeneration. *Curr Opin Neurobiol* 14(1):118–124.
5. Yiu G, He Z (2006) Glial inhibition of CNS axon regeneration. *Nat Rev Neurosci* 7(8):617–627.
6. Gianola S, Savio T, Schwab ME, Rossi F (2003) Cell-autonomous mechanisms and myelin-associated factors contribute to the development of Purkinje axon intracortical plexus in the rat cerebellum. *J Neurosci* 23(11):4613–4624.
7. Zagrebelsky M, Schweigreiter R, Bandtlow CE, Schwab ME, Korte M (2010) Nogo-A stabilizes the architecture of hippocampal neurons. *J Neurosci* 30(40):13220–13234.
8. Aloy EM, et al. (2006) Synaptic destabilization by neuronal Nogo-A. *Brain Cell Biol* 35(2-3):137–156.
9. Delekate A, Zagrebelsky M, Kramer S, Schwab ME, Korte M (2011) NogoA restricts synaptic plasticity in the adult hippocampus on a fast time scale. *Proc Natl Acad Sci USA* 108(6):2569–2574.
10. Lee H, et al. (2008) Synaptic function for the Nogo-66 receptor NgR1: Regulation of dendritic spine morphology and activity-dependent synaptic strength. *J Neurosci* 28(11):2753–2765.
11. Raiker SJ, et al. (2010) Oligodendrocyte-myelin glycoprotein and Nogo negatively regulate activity-dependent synaptic plasticity. *J Neurosci* 30(37):12432–12445.
12. Caroni P, Schwab ME (1988) Antibody against myelin-associated inhibitor of neurite growth neutralizes nonpermissive substrate properties of CNS white matter. *Neuron* 1(1):85–96.
13. Chen MS, et al. (2000) Nogo-A is a myelin-associated neurite outgrowth inhibitor and an antigen for monoclonal antibody IN-1. *Nature* 403(6768):434–439.
14. Huber AB, Weinmann O, Brösamle C, Oertle T, Schwab ME (2002) Patterns of Nogo mRNA and protein expression in the developing and adult rat and after CNS lesions. *J Neurosci* 22(9):3553–3567.
15. Hunt D, Coffin RS, Prinjha RK, Campbell G, Anderson PN (2003) Nogo-A expression in the intact and injured nervous system. *Mol Cell Neurosci* 24(4):1083–1102.
16. Josephson A, et al. (2002) Nogo-receptor gene activity: Cellular localization and developmental regulation of mRNA in mice and humans. *J Comp Neurol* 453(3):292–304.
17. Sillitoe RV, Joyner AL (2007) Morphology, molecular codes, and circuitry produce the three-dimensional complexity of the cerebellum. *Annu Rev Cell Dev Biol* 23:549–577.
18. Altman J (1972) Postnatal development of the cerebellar cortex in the rat. I. The external germinal layer and the transitional molecular layer. *J Comp Neurol* 145(3):353–397.
19. Nishiyama H, Linden DJ (2004) Differential maturation of climbing fiber innervation in cerebellar vermis. *J Neurosci* 24(16):3926–3932.
20. Simonen M, et al. (2003) Systemic deletion of the myelin-associated outgrowth inhibitor Nogo-A improves regenerative and plastic responses after spinal cord injury. *Neuron* 38(2):201–211.
21. Oertle T, et al. (2003) Nogo-A inhibits neurite outgrowth and cell spreading with three discrete regions. *J Neurosci* 23(13):5393–5406.
22. Smeyne RJ, et al. (1991) Dynamic organization of developing Purkinje cells revealed by transgene expression. *Science* 254(5032):719–721.
23. Metzger F, Kapfhammer JP (2000) Protein kinase C activity modulates dendritic differentiation of rat Purkinje cells in cerebellar slice cultures. *Eur J Neurosci* 12(6):1993–2005.
24. Lin YC, Koleske AJ (2010) Mechanisms of synapse and dendrite maintenance and their disruption in psychiatric and neurodegenerative disorders. *Annu Rev Neurosci* 33:349–378.
25. Kano M, Hashimoto K (2009) Synapse elimination in the central nervous system. *Curr Opin Neurobiol* 19(2):154–161.
26. Hashimoto K, Kano M (2003) Functional differentiation of multiple climbing fiber inputs during synapse elimination in the developing cerebellum. *Neuron* 38(5):785–796.
27. Chedotal A, Sotelo C (1992) Early development of olivocerebellar projections in the fetal rat using CGRP immunocytochemistry. *Eur J Neurosci* 4(11):1159–1179.
28. Mandolesi G, et al. (2009) Distribution of the SNAP25 and SNAP23 synaptosomal-associated protein isoforms in rat cerebellar cortex. *Neuroscience* 164(3):1084–1096.
29. Montani L, et al. (2009) Neuronal Nogo-A modulates growth cone motility via Rho-GTP/LIMK1/cofilin in the unlesioned adult nervous system. *J Biol Chem* 284(16):10793–10807.
30. Wills ZP, et al. (2012) The nogo receptor family restricts synapse number in the developing hippocampus. *Neuron* 73(3):466–481.
31. Foscarin S, et al. (2009) Overexpression of GAP-43 modifies the distribution of the receptors for myelin-associated growth-inhibitory proteins in injured Purkinje axons. *Eur J Neurosci* 30(10):1837–1848.
32. Wang X, et al. (2002) Localization of Nogo-A and Nogo-66 receptor proteins at sites of axon-myelin and synaptic contact. *J Neurosci* 22(13):5505–5515.
33. Niederöst B, Oertle T, Fritsche J, McKinney RA, Bandtlow CE (2002) Nogo-A and myelin-associated glycoprotein mediate neurite growth inhibition by antagonistic regulation of RhoA and Rac1. *J Neurosci* 22(23):10368–10376.
34. Li Z, Aizenman CD, Cline HT (2002) Regulation of rho GTPases by crosstalk and neuronal activity in vivo. *Neuron* 33(5):741–750.
35. Engert F, Bonhoeffer T (1999) Dendritic spine changes associated with hippocampal long-term synaptic plasticity. *Nature* 399(6731):66–70.
36. Maletic-Savatic M, Malinow R, Svoboda K (1999) Rapid dendritic morphogenesis in CA1 hippocampal dendrites induced by synaptic activity. *Science* 283(5409):1923–1927.
37. Smith SL, Otis TS (2003) Persistent changes in spontaneous firing of Purkinje neurons triggered by the nitric oxide signaling cascade. *J Neurosci* 23(2):367–372.
38. Dodd DA, et al. (2005) Nogo-A, -B, and -C are found on the cell surface and interact together in many different cell types. *J Biol Chem* 280(13):12494–12502.
39. Nie DY, et al. (2003) Nogo-A at CNS paranodes is a ligand of Caspr: Possible regulation of K(+) channel localization. *EMBO J* 22(21):5666–5678.
40. Schulz DJ (2006) Plasticity and stability in neuronal output via changes in intrinsic excitability: It's what's inside that counts. *J Exp Biol* 209(Pt 24):4821–4827.
41. Mandolesi G, et al. (2009) GluRdelta2 expression in the mature cerebellum of hotfoot mice promotes parallel fiber synaptogenesis and axonal competition. *PLoS ONE* 4(4):e5243.
42. Hashimoto K, et al. (2001) Roles of glutamate receptor delta 2 subunit (GluRdelta 2) and metabotropic glutamate receptor subtype 1 (mGluR1) in climbing fiber synapse elimination during postnatal cerebellar development. *J Neurosci* 21(24):9701–9712.
43. Miyazaki T, et al. (2006) Disturbance of cerebellar synaptic maturation in mutant mice lacking BSRPs, a novel brain-specific receptor-like protein family. *FEBS Lett* 580(17):4057–4064.
44. Watase K, et al. (1998) Motor discoordination and increased susceptibility to cerebellar injury in GLAST mutant mice. *Eur J Neurosci* 10(3):976–988.
45. Watanabe M (2008) Molecular mechanisms governing competitive synaptic wiring in cerebellar Purkinje cells. *Tohoku J Exp Med* 214(3):175–190.
46. Watanabe F, et al. (2008) Effects of FAK ablation on cerebellar foliation, Bergmann glia positioning and climbing fiber territory on Purkinje cells. *Eur J Neurosci* 27(4):836–854.
47. Sivasankaran R, et al. (2004) PKC mediates inhibitory effects of myelin and chondroitin sulfate proteoglycans on axonal regeneration. *Nat Neurosci* 7(3):261–268.
48. Kano M, et al. (1995) Impaired synapse elimination during cerebellar development in PKC gamma mutant mice. *Cell* 83(7):1223–1231.
49. Maeder CI, Shen K (2011) Genetic dissection of synaptic specificity. *Curr Opin Neurobiol* 21(1):93–99.
50. Margeta MA, Shen K (2010) Molecular mechanisms of synaptic specificity. *Mol Cell Neurosci* 43(3):261–267.
51. O'Connor TP, et al. (2009) Semaphorin 5B mediates synapse elimination in hippocampal neurons. *Neural Dev* 4:18.
52. Vanderhaeghen P, Cheng HJ (2010) Guidance molecules in axon pruning and cell death. *Cold Spring Harb Perspect Biol* 2(6):a001859.
53. Cesa R, et al. (2011) Eph receptors are involved in the activity-dependent synaptic wiring in the mouse cerebellar cortex. *PLoS ONE* 6(4):e19160.
54. Nishida K, Flanagan JG, Nakamoto M (2002) Domain-specific olivocerebellar projection regulated by the EphA-ephrin-A interaction. *Development* 129(24):5647–5658.
55. Hashimoto K, Ichikawa R, Kitamura K, Watanabe M, Kano M (2009) Translocation of a "winner" climbing fiber to the Purkinje cell dendrite and subsequent elimination of "losers" from the soma in developing cerebellum. *Neuron* 63(1):106–118.
56. Uemura T, et al. (2010) Trans-synaptic interaction of GluRdelta2 and Neurexin through Cbln1 mediates synapse formation in the cerebellum. *Cell* 141(5):1068–1079.
57. Santos Da Silva J, Schubert V, Dotti CG (2004) RhoA, Rac1, and cdc42 intracellular distribution shift during hippocampal neuron development. *Mol Cell Neurosci* 27(1):1–7.
58. Fischer M, Kaech S, Knutti D, Matus A (1998) Rapid actin-based plasticity in dendritic spines. *Neuron* 20(5):847–854.
59. Willi R, Aloy EM, Yee BK, Feldon J, Schwab ME (2009) Behavioral characterization of mice lacking the neurite outgrowth inhibitor Nogo-A. *Genes Brain Behav* 8(2):181–192.